



Antibacterial, self-adhesive guar gum/polyvinyl alcohol/tannic acid conductive hydrogels for flexible strain sensors

Noppanan PUTDON¹, Somnuk THEERAKULPISTUT², Rawit JITTHAM¹, and Pornnapa KASEMSIRI^{1,*}

¹Department of Chemical Engineering, Faculty of Engineering, Khon Kaen University, Khon Kaen 4002, Thailand

²Energy Management and Conservation Office, Faculty of Engineering, Khon Kaen University, Khon Kaen 40002, Thailand

*Corresponding author e-mail: pornkas@kku.ac.th

Received date:

21 January 2025

Revised date:

7 March 2025

Accepted date:

14 March 2025

Keywords:

Strain sensor;

Tannic acid;

Crosslinker

Abstract

In this research, a multifunctional strain sensor with antibacterial properties and self-adhesion capabilities was developed using guar gum (GG), polyvinyl alcohol (PVA), and tannic acid (TA). The incorporation of TA into GG-PVA hydrogel-based strain sensors was investigated to evaluate its effects on mechanical and electrical properties, self-adhesion, and antibacterial activities. The antibacterial activities against *Escherichia coli* (*E. coli*) and *Staphylococcus aureus* (*S. aureus*) were enhanced with the increasing content of TA. The adhesive strength was observed in the range of 1.20 ± 0.10 kPa to 5.05 ± 0.23 kPa, and the values tended to increase as TA content increased. The tensile strength significantly increased by up to 86.66% when 1.5% TA was incorporated into the hydrogel, followed by a slight increase with the addition of TA at higher contents. Consequently, the hydrogel strain sensor with 1.5% TA was selected to evaluate its sensing capability for limb movement. The sample exhibited reproducibility and stability of the signals during repeated movements. These properties highlight the potential of strain sensors with multifunctional capabilities for applications in wearable electronic devices.

1. Introduction

Multifunctional hydrogels with exceptional properties, including high mechanical strength, good electrical conductivity, self-adhesion, and antibacterial activity, have garnered significant attention due to their broad applications in biomedical fields, flexible electronics, and various other areas [1]. Conductive hydrogels have been developed and are widely used as strain sensors to detect external stimuli and convert them into measurable electrical signals, supporting applications in human motion monitoring and personal health diagnostics [2]. To fabricate conductive hydrogels, biopolymers are promising eco-friendly materials that have been widely used due to their low toxicity, abundance, and biodegradability [3]. Guar Gum (GG) is a biopolymer commonly obtained from wheat flour during the food production process. Insoluble GG is separated from wheat flour, and its sticky and flexible components, glutenin and gliadin, make it suitable for use as an adhesive [4]. GG has been used to prepare hydrogel-based strain sensors to enhance toughness and promote flexibility [5]. Recently, GG has also been blended with other polymers to achieve the desired properties such as polyvinyl alcohol (PVA) [6]. Deka *et al.* [7] observed that varying the ratio of GG blended with PVA could control swelling. As the weight percentage of PVA increased, the degree of interaction between PVA-PVA and PVA-GG molecules was enhanced due to the extensive hydrogen bonds formed between the blends. Over the past decade, PVA has been widely used as a hydrogel material due to its water solubility, chemical stability, biodegradability, and biocompatibility, which stem from the abundant -OH groups along its molecular chain

[8]. Besides designing the properties of hydrogels by varying the ratio of polymer blends, the use of crosslinkers is another approach to attain the desired properties. Tannic acid (TA), a natural phenolic compound, has been used as both a crosslinker and stabilizer for various biopolymers through the formation of hydrogen bonds between the polymer and the hydroxyl groups in its structure [9]. Wu *et al.* [10] studied that the addition of TA to PVA hydrogel enhanced antimicrobial properties and water retention capacity of hydrogel. Jaroenthai *et al.* [11] reported that incorporating TA into hydrogel-based strain sensors remarkably improved their tensile strength, self-adhesion properties, and conductivity. This enhancement highlights TA's ability to create the hydrogel's polymer network, making it more robust and versatile for sensing applications. Based on previous studies, research on hydrogel-based strain sensors often focuses on only two or three properties, such as electrical conductivity, mechanical strength, self-adhesion, and self-healing, to achieve optimal performance [12-14]. Consequently, studying the combination of self-adhesion, self-healing, antibacterial properties, electrical conductivity, and mechanical strength in hydrogel-based strain sensors could lead to wider applications.

In this study, the researchers investigated the effect of varying the blend ratio of GG and PVA to prepare hydrogel-based strain sensors. They then identified the optimal ratio of GG: PVA as the polymer matrix and studied the impact of adding TA on the sensor's self-adhesion, antibacterial activities, mechanical properties, and conductivity. The resulting strain sensor was applied to monitor joint movement, demonstrating its potential for wearable health monitoring and other flexible sensor applications.

2. Experiment

2.1 Materials

PVA with molecular weight of 1700 g·mol⁻¹ was acquired from TCI, Japan. GG was obtained from a supermarket in Khon Kaen, Thailand. TA was purchased from Loba Chemie Pvt. Ltd., India. Glycerol with purity of 99.50% was obtained from Kem Aus TM, Australia and Sodium carbonate (Na₂CO₃) with AR grade was purchased from QReCTM, New Zealand.

2.2 Preparation of GG-PVA hydrogel crosslinked with TA

Firstly, GG-PVA solution was prepared at GG: PVA weight ratios of 0:100, 80:20, 60:40 50:50, 40:60, and 20:80 and GG was dissolved by 50 mL of distilled water (DI water) at 80°C whereas PVA was dissolved by 20 mL of DI at 90°C for 1 h 30 min. The GG-PVA solution was mixed and then stirred at 60°C for 1 h 30 min, then poured into Petri dish and dried in an oven at 40°C for 8 h to obtain hydrogel. The GG-PVA hydrogel with the highest water retention capacity and shape stability was selected for further crosslinking with tannic acid. To prepare the GG-PVA crosslinked hydrogel, the TA solution (0.5, 1.5, 2, and 2.5%w/v) was adjusted to pH 8 by using sodium carbonate solution. After that, the TA solution (20 mL) was added to the GG-PVA solution and then stirred at 60°C for 3 h. The obtained solution was poured into a Petri dish and dried under the same conditions as mentioned above.

2.3 Characterization of GG-PVA crosslinked TA hydrogel's properties

2.3.1 FTIR analysis

The functional group of the hydrogel was tested by Fourier transform infrared spectroscopy (FTIR) with JASCO 4200 in Attenuated total reflection infrared (ATR) mode and the FTIR spectra were recorded with wavelength number range of 4000 cm⁻¹ to 500 cm⁻¹.

2.3.2 Mechanical properties of hydrogel

Mechanical properties of hydrogel were measured by Shimadzu universal testing machine at room temperature. The tensile strength samples were cut to 0.3 mm × 20 mm × 60 mm and tensile measurements were made at a tensile speed of 10 mm·min⁻¹. The shear strength test was used for studying the adhesion properties of hydrogel. The pig skin was cut to 20 mm × 60 mm, and a hydrogel size of 0.3 mm × 20 mm × 30 mm was placed between two pieces of the pig skin. The adhesion was tested using a pull rate of 10 mm·min⁻¹ and the shear strength was calculated by Equation (1). Both the tensile strength and shear strength values were averaged from five samples each.

$$\text{Shear strength (N·m}^{-2}, \text{ Pa)} = \frac{F}{A} \quad (1)$$

where F was maximum force (N), and A was cross-section area (m²)

2.3.3 Water retention of hydrogel

The water retention of the sample was measured following the method described by Hernández-Varela *et al.* [15]. The samples were cut into square pieces measuring 0.3 mm × 10 mm × 10 mm. Each sample was soaked in deionized water at room temperature until swelling equilibrium was reached. Excess water was removed using filter paper, and the hydrogel was immediately weighed. The size of the swollen hydrogel was recorded at soaking for 3 h. The water retention capacity was calculated using the formula:

$$\text{Water retention capacity (\%)} = \frac{W_s - W_i}{W_i} \times 100 \quad (2)$$

where W_s and W_i were the weight of the swollen hydrogel after soaking for 3 h and the dry weight of the hydrogel before soaking, respectively.

2.3.4 Electrical conductivity and relative resistance

The electrical resistance of the sample was measured using a two-probe KEITHLEY Model 2400 within a voltage range of 0 V to 12 V, and the electrical conductivity of the sample was calculated using Equation (3). The samples were cut to 0.3 mm × 2 mm × 2 mm. The average electrical conductivity was calculated from five samples.

$$\text{Electrical conductivity (S·m}^{-1}\text{)} = L \times \frac{R}{S} \quad (3)$$

where L was the distance between two adjacent probes (cm), R was the resistance of sample (Ω), and S was the cross-sectional area (cm²).

Real-time resistance changes in the strain sensor under various stimuli were measured using a Fluke 289 True RMS multimeter. The relative resistance was determined using Equation (4).

$$\text{Relative resistance (\%)} = \frac{(R - R_0)}{R_0} \times 100 \quad (4)$$

Where R₀ and R were the resistance without and with applied strain (Ω), respectively.

2.3.5 Antibacterial properties

The antibacterial properties of hydrogel were tested by the agar disc diffusion. The *E. coli* and *S. aureus* were spread on the solidified agar medium with a cotton swab stick. The samples were placed on the surface of an agar plate and incubated in an oven at 37°C for 12 h, and then a diameter of inhibition zone was measured.

3. Results and Discussion.

3.1 Water retention capacity of GG-PVA hydrogels

The water retention capacity of hydrogels is a vital property for biomedical applications. In strain sensor applications, all hydrogels demonstrate the ability to maintain their shape without breaking after soaking. This durability suggests their capability to endure daily tensile

forces, making them suitable for effective wearable sensing applications [16]. In addition, the high-water retention capacity of the hydrogel enables it to absorb electrolyte solutions, which further enhances its conductivity. Figure 1(a) illustrates the swollen shapes of GG-PVA hydrogels after soaking for 3 h. The samples with GG: PVA ratios of 0:100, 20:80, 40:60, 50:50, and 60:40 maintained post-soaking shape stability and exhibited water retention ranging from $200.32 \pm 19.08\%$ (for 0:100 of GG: PVA) to $813.00 \pm 35.19\%$ (for 60:40 of GG: PVA) shown in Figure 1(b). For the GG-PVA hydrogel with a ratio of 80:20, despite its highest water retention capacity ($1,040 \pm 63.02\%$), it failed to maintain shape stability after soaking. At high PVA content, the extensive hydrogen bonding between PVA molecules, along with its crystallinity, greatly enhanced the hydrogel's shape stability [17]. Since GG: PVA at 60:40 (GG-PVA hydrogel) exhibited the highest water retention capacity and its ability in maintaining shape stability during testing, it was selected for further investigation into the effect of TA crosslinking.

3.2 ATR-FTIR analysis of GG-PVA hydrogel crosslinked with TA

Figure 2(a) illustrates the absorbance spectra of raw materials such as TA, GG, and PVA. The spectrum of TA showed a broad band at 3261 cm^{-1} , corresponding to OH stretching vibrations. The carbonyl groups ($\text{C}=\text{O}$) were identified at 1695 cm^{-1} , while peaks at 1531 cm^{-1} and 1445 cm^{-1} indicated the presence of aromatic $\text{C}=\text{C}$ bonds. The aromatic $\text{C}-\text{O}$ symmetric stretching was observed at 1180 cm^{-1} and 1306 cm^{-1} [18]. GG exhibited characteristic peaks at 3319 cm^{-1} for O-H stretching, 2911 cm^{-1} for aliphatic C-H group stretching, 1405 cm^{-1} for C-H stretching and 1151 cm^{-1} for C-O-H [4]. The spectrum of PVA exhibited a peak at 3300 cm^{-1} corresponding to O-H stretching, 2920 cm^{-1} for CH stretching vibration in alkane, 1329 cm^{-1} for C-H deformation, 1083 cm^{-1} for C-O stretching of acetyl groups, and 840 cm^{-1} for C-C stretching vibrations [8,19]. The spectra of GG-PVA and GG-PVA crosslinked with TA at 0.5%w/v to 2.5%w/v are presented in Figure 2(b). The GG-PVA hydrogel exhibited the main characteristic peaks of both GG and PVA. For GG-PVA hydrogel crosslinked with TA, the ester group ($\text{C}=\text{O}$) of TA was shifted from 1695 cm^{-1} to 1647 cm^{-1} was observed, suggesting the interaction of hydrogen bonds between TA and the GG-PVA hydrogel [20].

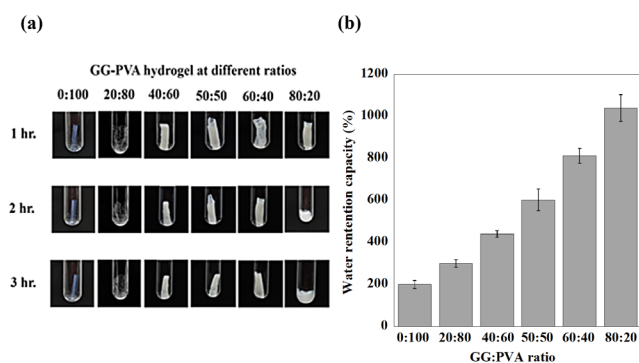


Figure 1. (a) Swollen shapes of all samples, and (b) histogram swelling ratio of hydrogel after soaking for 3 h.

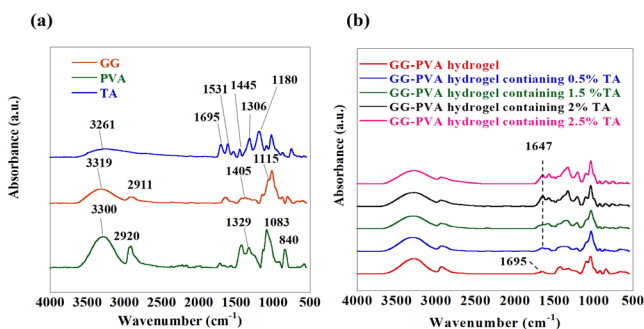


Figure 2. ATR-FTIR spectra (a) raw material, and (b) hydrogel at various TA content.

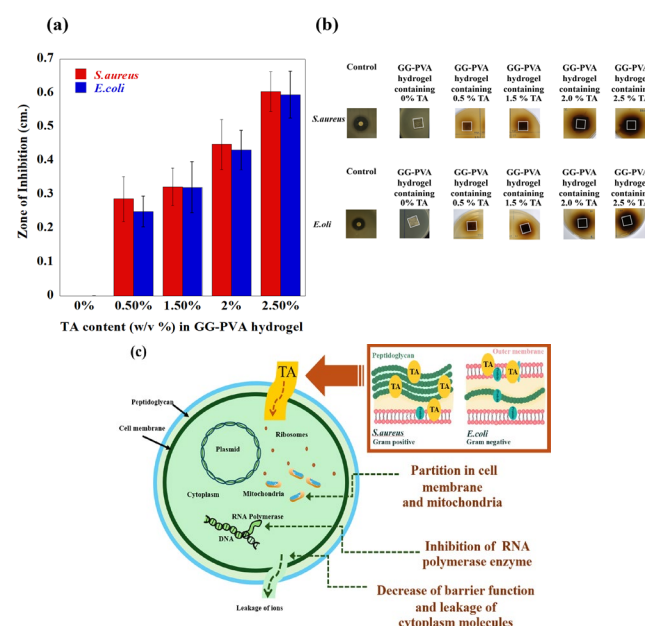


Figure 3. (a) Zone of inhibition diameter (mm), (b) Inhibition zone image of *E. coli* and *S. aureus*, and (c) Antibacterial mechanisms of TA.

3.3 Antibacterial activities of GG-PVA hydrogel cross linked with TA

Developing multifunctional hydrogels that integrate high sensitivity for health condition monitoring, strong self-adhesion, and remarkable antibacterial activity presents a promising approach for fabricating high-performance medical devices. These devices would not only enable effective health monitoring but also provide simultaneous medical treatment benefits. For this study, *E. coli* and *S. aureus* were selected as representative Gram-negative and Gram-positive bacteria, respectively. Figure 3 illustrates the antibacterial activities of the GG-PVA hydrogel crosslinked with TA. The inhibition zones for *E. coli* and *S. aureus* remarkably increased with increasing TA content as shown in Figure 3(a). The inhibition zone was found in the range of $0.25 \pm 0.07 \text{ cm}$ to $0.59 \pm 0.07 \text{ cm}$ for *E. coli* and $0.28 \pm 0.06 \text{ cm}$ to $0.60 \pm 0.06 \text{ cm}$ for *S. aureus* as depicted in Figure 3(b). The diffusion of TA through bacterial cell walls and internal membranes, inhibiting cellular metabolism [21]. This observation indicates that TA was more effective in suppressing the growth of Gram-positive bacteria than Gram-negative bacteria. The outer membrane of Gram-negative bacteria is composed of

lipopolysaccharides with a high chelating charge, while Gram-positive bacteria are primarily made up of peptidoglycan [22]. Consequently, Gram-negative bacteria are more resistant to microbial growth inhibition than Gram-positive bacteria. Possible antibacterial mechanisms of TA are illustrated in Figure 3(c). Based on the results, the GG-PVA hydrogel crosslinked with TA demonstrated strong antibacterial properties, making it effective in preventing infection and promoting healing in skin wounds.

3.4 Mechanical properties of GG-PVA hydrogel crosslinked with TA

Figure 4(a) shows adhesive strength of the samples. The self-adhesive property of the hydrogel is often the limitation of conventional hydrogel sensors, which require additional adhesives to attach the sensors to the skin or clothing. This not only enhances wearers' comfort but also improves the accuracy of the sensing signal [23]. The adhesive strength was found to range from 1.20 ± 0.10 kPa to 5.05 ± 0.23 kPa and increased with increasing TA content and the adhesive strength was comparable to that reported in a previous study where hydrogel composed PVA, sodium alginate and TA was crosslinked with borax yielding the adhesive strength to porcine skin of 3 kPa [14]. The incorporation of TA into the hydrogel strain sensor enhances its adhesive strength through interactions between the catechol groups of TA and the substrates. These interactions involve multiple mechanisms, including hydrogen bonding, covalent bonding, hydrophobic interactions, covalent crosslinking, π - π stacking, and cation- π interactions [11,24], which improve the sensor's self-adhesion capability. Furthermore, developing strain sensors from hydrogels with high stretchability and tensile strength is crucial for expanding their potential applications across a wide range of fields. Figure 4(b) shows the values of tensile strength in the range of 16.05 ± 1.97 to 33.62 ± 1.22 kPa. The incorporation of 1.5% TA significantly enhanced the tensile strength, achieving an increase of up to 86.66% compared to the neat sample. Beyond this, a slight increase in tensile strength was observed at TA concentrations of 2.0% to 2.5%. Increasing the TA content to an optimal level enhances the hydrogen bond interactions between TA and the gel matrix, resulting in a higher modulus and an effective energy-dissipating mechanism [11]. The obtained tensile strength was comparable to those reported in previous studies, such as polypyrrole- polyacrylamide hydrogel (25 kPa) [25], polydiacetylene-polyacrylic acid- Cr^{3+} (7 kPa) [26], poly (N-isopropyl acrylamide) functionalized Mxene (14 kPa) [27] and ionic conductive hydrogel (0.17 kPa) [28].

3.5 Electrical conductivity of GG-PVA hydrogel cross linked with TA

Based on previous study, the water within the hydrogel facilitates the ionization of TA, producing free hydrogen ions. These ions migrate through the polymer matrix under an applied voltage, thereby enhancing the conductivity of the hydrogel strain sensor [28]. Table 1. presents the electrical conductivity values of the hydrogel strain sensor. The electrical conductivity increased with the incorporation of TA into the hydrogel up to 1.5%, after which it began to decrease. At higher TA concentrations, the increased crosslinking density of the hydrogel

leads to a more tightly interconnected polymer network. This denser structure reduces the size and amount of free volume within the hydrogel matrix, restricting the movement of water molecules and solvated ions [29]. The electrical conductivity of the GG-PVA hydrogel crosslinked with 1.5% TA was comparable to those reported in previous studies, such as polyacrylamide hydrogel containing decorated hydroxyethyl cellulose with AgNPs ($0.08 \text{ S}\cdot\text{m}^{-1}$) [30], and nanocomposite hydrogel-based CMC-PVA-Glycerol-Borax containing AgNPs ($0.22 \text{ m S}\cdot\text{m}^{-1}$) [31].

3.6 Strain-sensing performance of GG-PVA hydrogel crosslinked with TA

Based on the results, the hydrogel incorporated with 1.5% TA exhibited excellent antibacterial activity and mechanical properties, along with the highest electrical conductivity. Therefore, it was tested for its strain-sensing performance. The strain-sensing performance of the sample was evaluated by monitoring limb movement, as shown in Figure 5. The strain sensor, measuring $0.3 \text{ mm} \times 10 \text{ mm} \times 10 \text{ mm}$, was directly placed on the shoulder of the robot model and connected to a multimeter using wires. The shoulder was moved from its initial position to 90° at intervals of 4 s, as shown in Figure 5(a). The reproducibility and stability of the signals during repeated movements were observed, demonstrating the sample's good stability in detecting motion, as shown in Figure 5(b). The motion signal was generated by variation in the sensor's electrical resistance and the resulting current. In the relaxed state, the sensor exhibited higher resistance, leading to a lower current. When the sensor was bent, the deformation reduced the resistance by enhancing the contact between conductive pathways, allowing more charge carriers to flow. Consequently, the current increased and reached its peak at maximum bending [11,32].

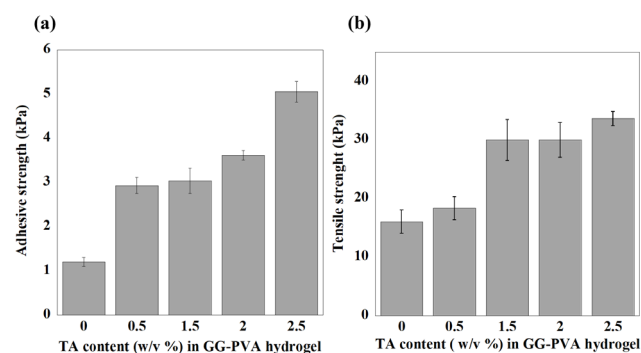


Figure 4. (a) Adhesive strength, and (b) Tensile strength of hydrogel with different concentration of TA.

Table 1. Conductivity value of hydrogel strain sensor with different TA concentration.

Content of TA in GG-PVA hydrogel [%w/v]	Conductivity [$\text{S}\cdot\text{m}^{-1}$]
0	$0.004 \pm 1.79 \times 10^{-5}$
0.5	0.011 ± 0.001
1.5	0.053 ± 0.002
2	0.047 ± 0.005
2.5	0.028 ± 0.002

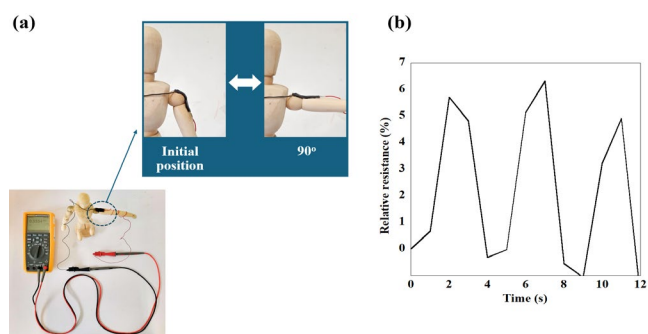


Figure 5. (a) Hydrogel strain sensor with 1.5% of TA in monitoring limb movement, and (b) application of hydrogel with 1.5% TA as a strain sensor.

4. Conclusions

A multifunctional strain sensor with antibacterial properties and self-adhesion capabilities was successfully developed using TA as a crosslinker. The effect of incorporating TA at 0.5% to 2.5 % was investigated. The antibacterial activity against *E. coli* and *S. aureus* improved with increasing TA content. The adhesive strength ranged from 1.20 ± 0.10 kPa to 5.05 ± 0.23 kPa, demonstrating a consistent increase with higher TA concentrations. The tensile strength of the hydrogel increased significantly, with an 86.66% improvement observed at 1.5% TA, followed by a slight enhancement at higher TA contents. The highest tensile strength was recorded at 33.62 ± 1.22 kPa, with a stretchability of 251.64%. Based on these findings, the hydrogel strain sensor with 1.5% TA was selected to evaluate its sensing performance for limb movements. The sample exhibited excellent reproducibility and signal stability during repeated motions, underscoring its potential for applications in wearable electronic devices. These findings highlight the significant promise of multifunctional strain sensors for advanced wearable technology.

Acknowledgement

This work was supported by Faculty of Engineering, Khon Kaen University (Fund code: M-Eng.-CHE. -10/2568) and Fundamental Fund of Khon Kaen University (The research on "Product development and investment feasibility study of innovations from waste and by-product from agricultural production" by the Faculty of Engineering at Khon Kaen University has received funding support from the National Science, Research and Innovation Fund (NSRF), Thailand).

References

- [1] Y. Zhang, G. Lu, C. Yan, J. Luo, X. Zhou, and J. Wang, "Fabrication of flexible accelerated-wound-healing chitosan/dopamine-based bilayer hydrogels for strain sensors," *International Journal of Biological Macromolecules*, vol. 253, p. 127395, 2023.
- [2] G. Li, C. Li, G. Li, D. Yu, Z. Song, H. Wang, X. Liu, H. Liu, and W. Liu "Development of conductive hydrogels for fabricating flexible strain sensors," *Nano Micro small*, p. 2101518, 2021.
- [3] C. Cui, Q. Fu, L. Meng, S. Hao, R. Dai, and J. Yang, "Recent progress in natural biopolymers conductive hydrogels for flexible wearable sensors and energy devices: Materials, structures, and performance," *Applied Bio Material*, no. 4, p. 85-121, 2021.
- [4] A. Ounkaew, P. Kasemsiri, N. Srichaingsa, K. Jetsrisuparb, J. T. N. Knijnenburg, M. Okhawilai, S. Hiziroglu, and S. Theerakulpisut, "Multifunctional gluten/guar gum copolymer with self-adhesion, self-healing, and remolding properties as smart strain sensor and self-powered device," *Express Polymer Letters*, vol. 16, no. 6, pp. 607-623, 2022.
- [5] Y. Li, Y. Liu, H. Lui, S. Yu, Z. Ba, M. Liu, S. Ma, and L. B. Xing, "Design of stretchable and conductive self-adhesive hydrogels as flexible sensors by guar-gum-enabled dynamic interactions," *Langmuir*, vol. 40, no. 19, pp. 10305-10312, 2024.
- [6] J. S. Kim, J. S. Kim, J. Kim, S. M. Lee, M. R. Woo, D. W. Kim, J. O. Kim, H. G. Choi, and S. G. Jin "Development of guar gum-based dual-layer wound dressing containing *Lactobacillus plantarum*: Rapid recovery and mechanically flexibility," *International Journal of Biological Macromolecules*, vol. 221, p. 1572-1579, 2022.
- [7] R. Deka, S. Sarma, P. Patar, P. Gogoi, and J. K. Sarmah, "Highly stable silver nanoparticles containing guar gum modified dual network hydrogel for catalytic and biomedical applications," *Carbohydrate Polymers*, vol. 248, p. 116786, 2020.
- [8] K. H. Hong, "Polyvinyl alcohol/tannic acid hydrogel prepared by a freeze-thawing process for wound dressing applications," *Polymer Bulletin*, vol. 74, no. 7, pp. 2861-2872, 2017.
- [9] C. Chen, H. Yang, X. Yang, and Q. Ma, "Tannic acid: A crosslinker leading to versatile functional polymeric networks: A review," *RCS Advances*, vol. 12, p. 7689, 2022.
- [10] W. Wu, L. Shi, K. Qian, J. Zhou, T. Zhao, S. Thaiboonrod, M. Miao, and X. Feng "Synergistic strengthening of PVA ionic conductive hydrogels using aramid nanofibers and tannic acid for mechanically robust, antifreezing, water-retaining and antibacterial flexible sensors," *Journal of Colloid And Interface Science*, vol. 654, pp. 1260-1271, 2024.
- [11] N. Jaroenthai, N. Srikhao, P. Kasemsiri, M. Okhawilai, S. Theerakulpisut, H. Uyama, and P. Chindapasirt "Optimization of rapid self-healing and self-adhesive gluten/guar gum crosslinked gel for strain sensors and electronic devices," *International Journal of Biological Macromolecules*, vol. 253, p. 127401, 2023.
- [12] Y. Wen, L. Y. Zeng, X. C. Wang, H. M. Chen, X. C. Li, H. L. Ni, W. H. Yu, Y. F. Bai, and P. Hu "Conductive hydrogel based on dual-network structure with high toughness, adhesion, self-healing and anti-freezing for flexible strain sensor," *Next Materials*, vol. 6, p. 100436, 2025.
- [13] L. Zhao, Z. Ren, X. Liu, Q. Ling, Z. Li, and H. Gu, "A multifunctional, self-healing, self-adhesive, and conductive sodium alginate/poly(vinyl alcohol) composite hydrogel as a flexible strain sensor," *Applied Materials And Interfaces*, vol. 13, no. 9, p. 11344-11355, 2021.
- [14] L. Zhao, T. Ke, Q. Ling, J. Liu, Z. Li, and H. Gu, "Multifunctional ionic conductive double-network hydrogel as a long-term flexible strain sensor," *Applied Polymer Material*, vol. 3, no. 11, p. 5494-5508, 2021.
- [15] J. D. Hernández-Varela, J. J. Chanona-Pérez, R. Foruzanmehr, and D. I. Medina, "Assessing the reinforcement effect by response

- surface methodology of holocellulose from spent coffee grounds on biopolymeric films as food packaging materials,” *Biopolymers*, vol. 115, no. 5, p. 23585, 2024.
- [16] W. Zhao, Z. Lin, X. Wang, Z. Wang, and Z. Sun, “Mechanically interlocked hydrogel–elastomer strain sensor with robust interface and enhanced water—retention capacity,” *Gels*, vol. 8, no. 10, p. 625, 2022.
- [17] X. Liang, H. J. Zhong, H. Ding, B. Yu, X. Ma, X. Liu, C. M. Chong, and J. He, “Polyvinyl alcohol (PVA)-based hydrogels: Recent progress in fabrication, properties, and multifunctional applications,” *Multidisciplinary Digital Publishing Institute*, vol. 16, p. 2755, 2024.
- [18] Z. Xia, A. Singh, W. Kiratitanavit, R. Mosurkal, J. Kumar, and R. Nagarajan, “Unraveling the mechanism of thermal and thermo-oxidative degradation of tannic acid,” *Thermochimica Acta*, vol. 605, p. 77-85, 2015.
- [19] I. M. Jipa, A. Stoica, M. Stroescu, L. M. Dobre, T. Dobre, S. Jinga, and C. Tardei, “Potassium sorbate release from poly (vinyl alcohol)-bacterial cellulose films,” *Chemical Papers*, vol. 66, no. 2, p. 138-143, 2012.
- [20] R. Sharma, V. Singh, and M. Ahuja, “Evaluation of modified guar gum as polymer for electrospun nanofibrous film,” *Polymers for Advanced Technologies*, vol. 36, p. 70062, 2025.
- [21] M. Cheng, L. Hu, G. Xu, P. Pan, Q. Liu, Z. Zhang, Z. He, C. Wang, M. Liu, L. Chen, and J. Chen, “Tannic acid-based dual-network homogeneous hydrogel with antimicrobial and pro-healing properties for infected wound healing,” *Colloids and Surfaces B: Biointerfaces*, vol. 227, p. 113354, 2023.
- [22] A. Sharma, C. Verma, S. Mukhopadhyay, A. Gupta, and B. Gupta, “Development of sodium alginate/glycerol/tannic acid coated cotton as antimicrobial system,” *International Journal of Biological Macromolecules*, vol. 216, pp. 303-311, 2022.
- [23] Y. Luo, J. Li, Q. Ding, H. Wang, C. Liu, and J. Wu, “Functionalized hydrogel-based wearable gas and humidity sensors,” *Nano-Micro Letters*, vol. 15, p. 136, 2023.
- [24] M. Liao, Y. Zhao, Y. Pan, J. Pan, Q. Yao, S. Zhang, H. Zhao, Y. Hu, W. Zheng, W. Zhou, and X. Dong, “A good adhesion and antibacterial double-network composite hydrogel from PVA, sodium alginate and tannic acid by chemical and physical cross-linking for wound dressings,” *Material for life Sciences*, vol. 58, no. 13, pp. 5756-5772, 2023.
- [25] R. Chen, X. Xu, D. Yu, C. Xiao, M. Liu, J. Huang, T. Mao, C. Zheng, Z. Wang, and X. Wu, “Highly stretchable and fatigue resistant hydrogels with low Young’s modulus as transparent and flexible strain sensors,” *Journal of Material Chemistry C*, vol. 6, no. 41, pp. 11193-11201, 2018.
- [26] V. K. Rao, N. Shauloff, X. M. Sui, H. Daniel Wagner, R. Jelinek, and R. Jelinek, “Polydiacetylene hydrogel self-healing capacitive strain sensor,” *Journal of Material Chemistry C*, vol. 8, no. 18, pp. 6034-6041, 2020.
- [27] F. Hao, L. Wang, B. Chen, L. Qiu, J. Nie, and G. Ma, “Bifunctional smart hydrogel dressing with strain sensitivity and NIR-responsive performance,” *Applied Materials and Interfaces*, vol. 13, no. 39, pp. 46938-46950, 2021.
- [28] J. Gao, Z. Yu, H. Xue, T. Zhang, J. Gu, and F. Huang, “Highly conductive and sensitive alginate hydrogel strain sensors fabricated using near-field electrohydrodynamic direct-writing process,” *International Journal of Biological Macromolecules*, vol. 282, p. 136802, 2024.
- [29] I. Hussain, X. Ma, L. Wu, and Z. Luo, “Hydroxyethyl Cellulose-based electrically conductive mechanically resistant strain-sensitive self-healing hydrogels,” *Research square*, p. 21203, 2021.
- [30] X. Wang, Z. Wang, X. Wang, L. Shi, and R. Ran, “Preparation of silver nanoparticles by solid-state redox route from hydroxyethyl cellulose for antibacterial strain sensor hydrogel,” *Carbohydrate Polymers*, vol. 257, p. 117665, 2021.
- [31] I. Taesuwan, A. Ounkaew, M. Okhawilai, S. Hiziroglu, W. Jareenboon, P. Chindapasirt, and P. Kasemsiri, “Smart conductive nanocomposite hydrogel containing green synthesized nanosilver for use in an eco-friendly strain sensor,” *Cellulose*, vol. 29, no. 1, pp. 273-286, 2022.
- [32] J. Tang, Y. Wu, S. Ma, T. Yan, and Z. Pan, “Sensing mechanism of a flexible strain sensor developed directly using electrospun composite nanofiber yarn with ternary carbon nanomaterials,” *iScience*, vol. 25, no. 10, 2022..